



OPEN Optimizing focused very-high-energy electron beams for radiation therapy based on Monte Carlo simulation

Chaofan An¹, Wei Zhang¹, Zeyi Dai¹, Jia Li¹, Xiong Yang², Jike Wang¹ & Yuancun Nie¹✉

A TOPAS-based optimization program has been developed to precisely concentrate the dose of focused very-high-energy electron (VHEE) beams on deep-seated targets. This is accomplished by optimizing the magnetic gradients, positions, and number of quadrupole magnets within TOPAS. Using only three quadrupole magnets, the program focuses 250 MeV VHEE beams to achieve a maximum dose position deeper than 17 cm, while maintaining entrance and exit doses within 25% and limiting the lateral dimensions to ≤ 1 cm at the maximum dose location. The linear relationship between the magnetic gradient of the last quadrupole magnet and the maximum dose position enables dose location adjustments through gradient variation. Multiple positions were validated in TOPAS with errors within 1%. The spread-out electron peak (SOEP) is achieved by combining two VHEE beams with different maximum dose positions using the differential evolution method, covering a target depth of 12–17 cm and attaining a dose flatness better than 99%. This pioneering program imposes constraints on entrance dose, exit dose, maximum dose position, and the lateral dimensions of dose deposition at the maximum dose position within phantom. This program may be a promising tool in the applications of focused VHEE in highly conformal treatment plans based on TOPAS.

Keywords Focused VHEE, FLASH-radiotherapy, Spread-out electron peak (SOEP)

For radiation therapy targeting deep-seated tumors, the rays need to penetrate 15–30 cm into the body¹. Very-high-energy Electron (VHEE) Beams referring to electron beams with energies ranging from 50 to 250 MeV, were first proposed for use in radiotherapy in 2000². VHEE beams provide adequate penetration to treat lesions at typical clinical depths and offer comparable lateral beam penumbra to state-of-the-art megavolt photon radiotherapy^{2–4}. VHEE beams also deliver similar, and sometimes superior, target coverage^{5–8} compared to protons⁹ and exhibit reduced susceptibility to tissue inhomogeneities^{8–11}.

FLASH radiation therapy requires the delivery of ultra-high dose rates (> 40 Gy/s) on sub-second time scale to damage tumor cells while reducing toxic effects to healthy tissue compared to conventional radiotherapy^{3,12–17}. VHEE beams are regarded as potential candidates for realizing deep-tumor FLASH radiotherapy in the near future¹⁸. FLASH radiotherapy based on VHEE, with sufficiently high beam energies, can provide dosimetric plans of comparable quality to FLASH radiotherapy based on transmission proton and can serve as a lighter particle alternative to protons³. FLASH parameters for VHEE radiotherapy has been explored and a benchmark for evaluating its FLASH dose rate performance has been successfully developed¹⁹.

For the widespread implementation of VHEE radiotherapy, it is essential to control the VHEE dose concentration in the target area and ideally provide highly conformal treatment plans to deliver FLASH dose rates. The longitudinal distribution of the parallel VHEE beam does not exhibit a Bragg peak. Therefore, the dose integrated over the transverse dimensions (x and y) also lacks a Bragg peak. Quadrupole magnets may be employed to focus electron beams for achieving conformal FLASH VHEE treatment, which concentrates the dose in the tumor target area and disperses it over a larger volume, thereby reducing the entrance and exit dose^{9,20–22}. While focusing can alter the transverse dose distribution, it does not change the integrated dose distribution over the x and y dimensions. As a result, the integral dose to healthy tissue along the z -axis remains constant, while the transverse dose density is diluted on the proximal or distal side from the focus. The use of focused VHEE beams provides a method for rapidly delivering target dose distributions. FLASH effect may be

¹The Institute for Advanced Studies, Wuhan University, Wuhan 430072, Hubei Province, China. ²Department of Radiation Oncology, Renmin Hospital of Wuhan University, Wuhan 430060, Hubei Province, China. ✉email: nieyuancun@whu.edu.cn

reduced by spot scanning or mechanical gantry motion^{20,23,24}. To date, most published VHEE treatment plans assume that using focused VHEE may eliminate the need for spot scanning or gantry motion^{8,19,20,25}, making it more suitable for FLASH radiotherapy. By using quadrupole magnets to focus VHEE beams with energies above 200 MeV, the maximum dose position on the axis can reach a depth of ≥ 15 cm, achieving the goal of treating deep-seated and highly heterogeneous tumors^{1,9,21}.

The tumor has a specific volume, and during radiation therapy, it is necessary for the radiation to encompass such a specific target area. Bortfeld and Schlegel²⁶ used multiple proton beams of varying energies, and adjusted their weights to spread-out the peak of the proton beam coverage over the tumor area. Similarly, accumulating VHEE beams of the same energy with different coefficients and peak dose positions can spread-out electron peak (SOEP)¹.

Whitmore combined Elegant²⁷ optimization results with Twiss parameter²⁸ analysis to predict the focusing position in a water phantom. The results optimized in Elegant under vacuum conditions may differ from those in water. The predicted position differed by 1–2 cm from the focusing dose position obtained through Monte Carlo simulations in TOPAS²⁹ using the beamline setup. This study aims to develop a TOPAS-based program to optimize the focusing of VHEE beams to concentrate the dose on the target area. The program includes three functions: 1. VHEE beams are focused using quadrupole magnets. 2. The coefficients of each beam are calculated to cover the deep target region with spread-out electron peaks (SOEP). 3. Time-variant SOEP is calculated in TOPAS to prepare for future research on conformal treatment planning with VHEE beams. This program optimizes the focusing of VHEE beams to more accurately control the maximum dose position within the target area, while also managing the entrance dose, exit dose, the lateral dimensions of dose deposition at the maximum dose position. This program uses the differential evolution method to solve the spread-out electron peak (SOEP), achieving the desired dose flatness with fewer beams.

Results

Optimization using three quadrupole magnets

Using the optimization program, VHEE beams are focused to irradiate a water phantom, and the parameters of the resulted dose distribution within the phantom are used as optimization objectives. Details of the optimization process to achieve the required beam characteristics can be found in the “Focused VHEE” section of the “Methods”. It is possible to effectively control the focusing of VHEE beams in a water phantom, and optimize the maximum dose delivery to the target location.

Considering practical applications where a fixed beamline is used and aiming to minimize errors arising from machine instability during radiation therapy, it is preferable to control the beams using fewer variables. To focus 250 MeV VHEE beams using three quadrupole magnets, the positions of the components are fixed and the magnetic gradients of the quadrupole magnets are set to T2 and T3, as specified in the “Method” section. The program is used to optimize the magnetic gradient T1 of the last quadrupole magnet and to collect z' corresponding to the position of the maximum dose. The specific parameters of the beamline are detailed in Supplementary Table S1, and the parameters of the 50 data points are listed in Supplementary Table S2. Utilizing linear regression, the corresponding relationship is shown in Fig. 1(a). Based on the fitting results, the specific parameters of the magnetic gradients for the target positions at 12 cm, 14 cm, and 16 cm are listed in

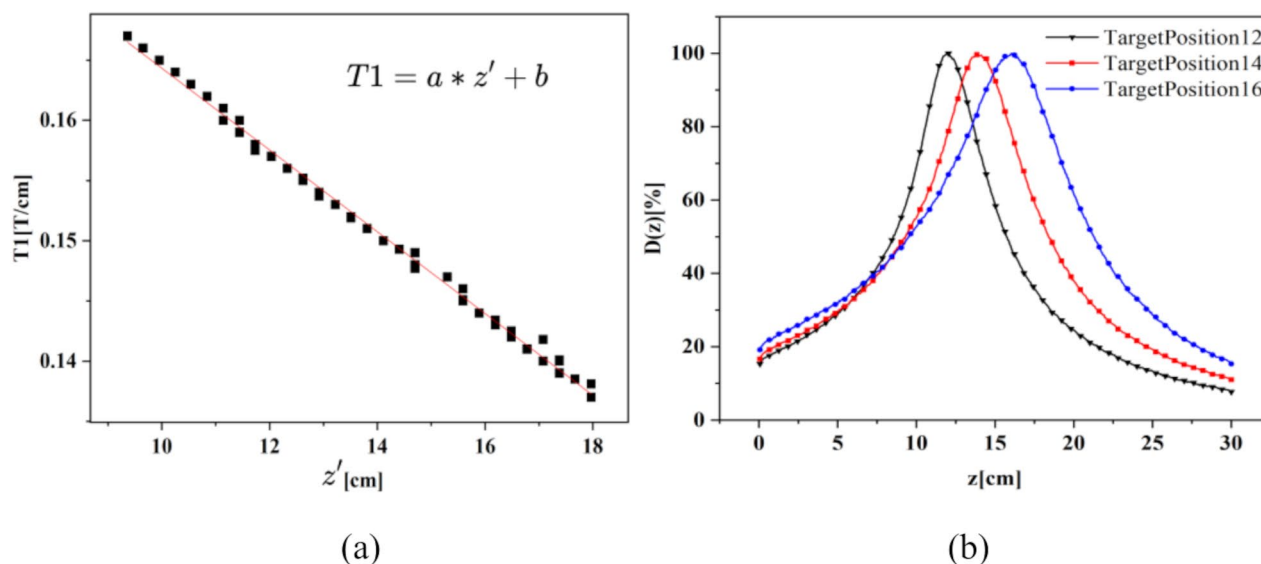


Fig. 1. (a) The linear fit between the position of the maximum dose and the gradient of the last quadrupole magnet is provided, $a = -0.0034 \pm 2.9249E - 5(T/cm^2)$, $b = 0.19828 \pm 4.1639E - 4(T/cm)$, adjusted $R^2 = 0.996$. (b) Dose distribution results obtained from TOPAS simulations with 10^6 particles for target positions at 12 cm, 14 cm, and 16 cm.

Parameter	z_I (cm)	D_{ent} (%)	D_{exit} (%)
TargetPosition12	11.92	15.3	7.68
TargetPosition14	13.89	16.66	11.02
TargetPosition16	16.05	19.16	15.33

Table 1. The positions of the maximum dose, as well as the entrance and exit relative doses, obtained using TOPAS simulations with 10^6 particles for target positions at 12 cm, 14 cm, and 16 cm.

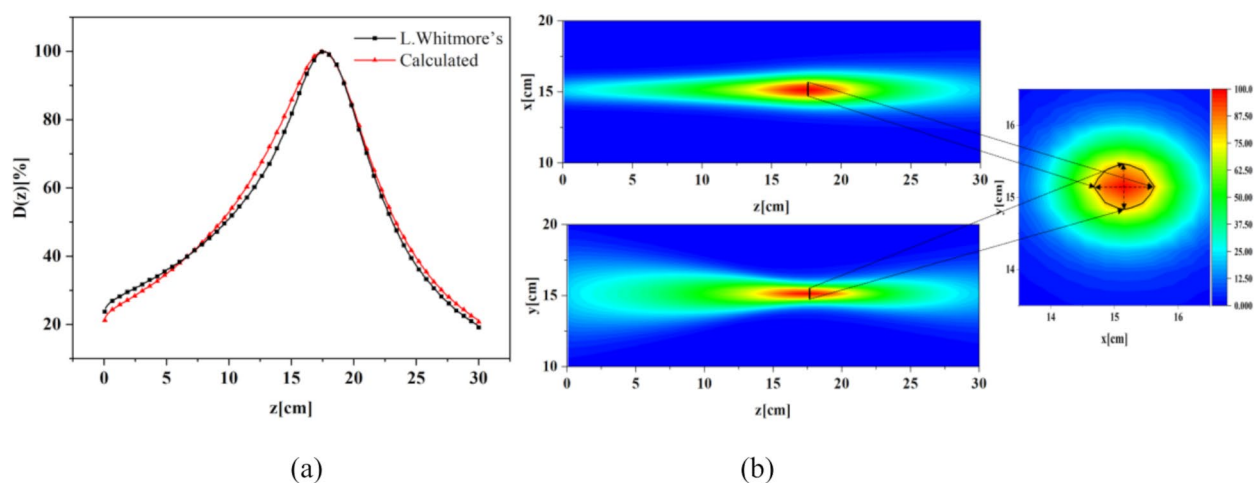


Fig. 2. (a) Comparison of the simulated dose distribution along the axis in the water phantom with L. Whitmore's results at 250 MeV¹. (b) Lateral dose distribution results corresponding to the position of the maximum dose at 17.5 cm.

Parameter	z_I (cm)	σ_x (cm)	σ_y (cm)	D_{ent} (%)
L.Whitmore_250MeV	17.4	0.84	0.54	25
Calculated_250MeV	17.5	0.96	0.63	21.23

Table 2. Simulation results of 250 MeV VHEE beam using TOPAS compared with that of L. Whitmore¹, including entrance dose along the axis, position of maximum dose, and corresponding beam sizes of σ_x and σ_y .

Supplementary Table S3. 10^6 particles are hence used in Monte Carlo simulations. Dose distributions along the central axis of the water phantom is shown in Fig. 1(b). The error in the maximum dose position is less than 1%. Dose distributions corresponding to the 3 maximum dose positions are detailed in Supplementary Fig. S1, Fig. S2 and Fig. S3, respectively. Entrance and exit dose results are provided in Table 1.

The optimization program was used to focus the VHEE beam, and the T1 value corresponding to 17.4 cm was calculated based on the linear regression curve. Three quadrupole magnets are used to focus the 250 MeV VHEE beam on a water phantom, with beamline settings as detailed in the “Methods” section. A maximum on-axis dose deposition at 17.5 cm in the water phantom was yielded by the Monte Carlo simulation using 10^7 particles, with a positional error of approximately 0.59%. The obtained dose distribution along the axis is comparable with the results of Whitmore¹, who used four quadrupole magnets to focus a 250 MeV VHEE beam, as shown in Fig. 2(a). Detailed comparison results are provided in Table 2. The lateral dose distribution corresponding to the maximum dose position at 17.5 cm is illustrated in Fig. 2(b).

SOEP

The optimization program has been used to spread-out the dose distribution region of the 250 MeV focused VHEE beams in water phantom, where the position of spread-out electron peak ranges from 12 to 17 cm along the axis of the phantom. The purpose is to calculate the coefficients (a_1 and a_2) for each beam used to achieve a flat longitudinal dose distribution in the specified area. Flatness exceeding 99% can be ensured by adjusting the magnetic gradients of the quadrupole magnets twice. The calculation method is described in the “Calculate SOEP” section of the “Methods”. The optimized results are shown in Fig. 3(a), with detailed results provided in Table 3. In TOPAS, the magnetic gradients of the quadrupole magnets are varied over time to spread-out

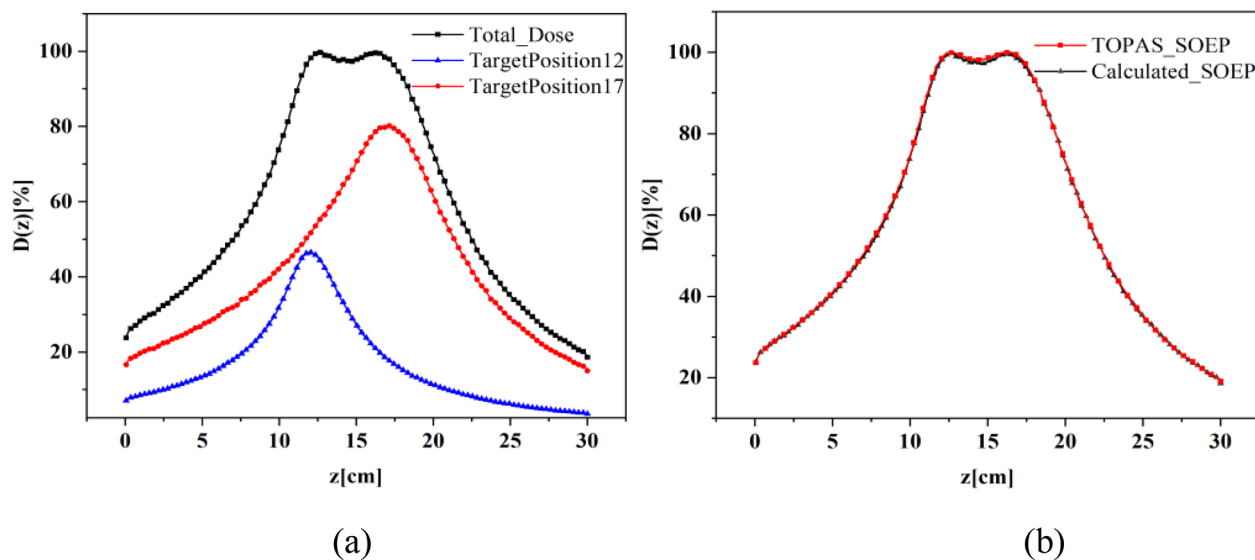


Fig. 3. (a) Dose distributions for SOEP were calculated using two beams with target positions at 12 cm and 17 cm. (b) The calculated SOEP and the time-variant SOEP obtained from TOPAS are compared (The time-variant SOEP obtained from TOPAS simulations is used to validate the accuracy of the calculated SOEP).

Parameter	Value	Unit
a_1	0.3484	/
a_2	0.8790	/
<i>flatness</i>	99.14	%

Table 3. Coefficients and flatness values calculated via “Calculate SOEP”.

electron peak. Monte Carlo simulations are performed to obtain the dose distribution in the water phantom and to verify the accuracy of the beam coefficients calculated by “Calculate SOEP”. The calculated SOEP and the time-variant SOEP obtained from TOPAS are compared in Fig. 3(b). In TOPAS, 12,274,000 particles were used to simulate the formation of a spread-out electron peak (SOEP) by VHEE beams in a water phantom. The simulation includes the longitudinal dose distribution and the lateral dose distributions at the entrance, exit, and maximum dose positions, as shown in Fig. 4.

Discussion

The optimization program was initially designed for focusing VHEE beams to treat deep-seated tumors. However, with modifications to beam energy, quadrupole magnet gradients, and quadrupole magnet sizes, it can also be applied to optimize the design of other particle beams platforms for focusing purposes. Focused VHEE beams can also be used to treat tumors at shallower depths by targeting different depth regions. Future research should investigate the relationship between the focusing state of VHEE beams and the penumbra.

This study optimized the “Focused VHEE” section based on parameter ranges derived from previous research of Whitmore¹. The following constraints were applied: quadrupole magnet gradient not exceeding 27 T/m¹, quadrupole magnet spacing not less than 25 cm²⁰, and drift section length not exceeding 2 m¹. The dimensions of each quadrupole magnet are 40 cm × 40 cm × 24 cm (external size), and the medium is set to air in TOPAS. Future research will need to incorporate vacuum chambers and other components into the optimization program’s model based on the actual specifications of the quadrupole magnets, and to impose constraints on the magnets’ apertures.

In this study, when optimizing the distance between the last quadrupole magnet and the water phantom, optimization parameter was set using distance similar to those in the previous works^{1,20}. This approach was adopted to validate the accuracy of the results. Clinical trial and preclinical settings have not yet been considered. The next step will be to integrate clinical settings and incorporate additional detailed configurations for simulation. To check the capability of our program, a recent optimization has been performed, which includes increasing L1 to 77 cm and setting the maximum dose position at 16.34 cm. The preliminary optimization results can be found in Supplementary Table S4, Supplementary Fig. S4, and Supplementary Table S5. Reducing the entrance dose to 25% is the next ongoing optimization goal.

In this study, the phantom material used is water. With the optimization program, by simply changing the material and shape of the target, it is possible to calculate the dose distribution of focused VHEE beams in other

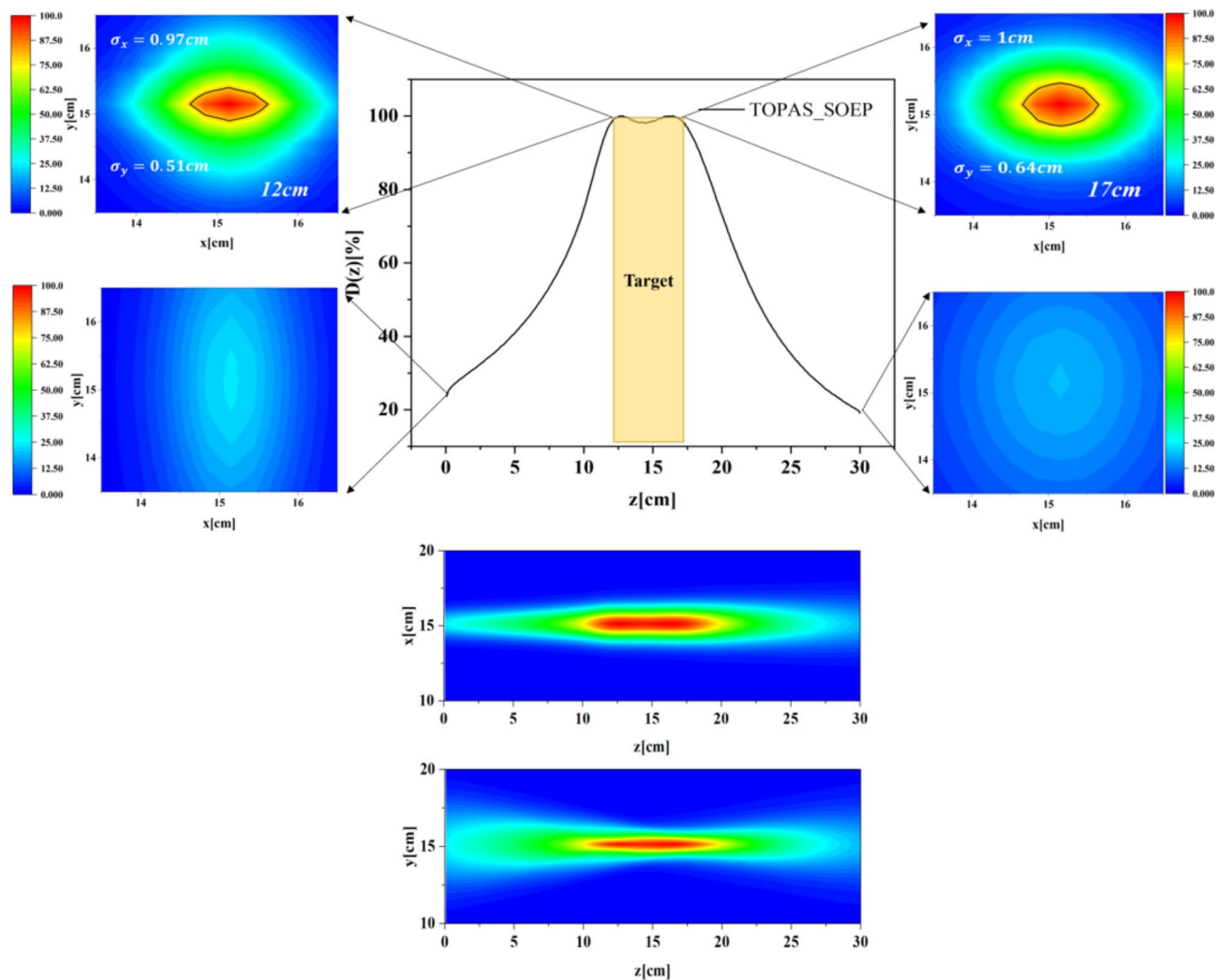


Fig. 4. Longitudinal dose distribution and lateral dose distributions at the entrance, exit, and the point of maximum dose in the water phantom.

targets. Future research will focus on lower-energy electron beams for treating deep-seated tumors in radiation therapy in order to lower the cost.

When using SOEP beams for lateral scanning irradiation, the dose overlap region between points in the lateral direction is related to the lateral dose fall-off gradient of an individual SOEP beam. Such SOEP beams are practical to treat certain tumors with proper sizes. However, depth conformity will be compromised when the scanned target areas are comparable to the beam size before focusing. This is due to the dose superposition effects occurring before and after the focal spot as reported before³⁰. The current optimization is based on the same beam sizes as in previous studies¹. In the future, optimization of the lateral dose region of the SOEP beam will be enhanced.

Conclusions

This study is based on Monte Carlo simulations and establishes a model in TOPAS that includes quadrupole magnets and a water phantom. To compare with L. Whitmore's¹ results of focused 250 MeV VHEE beams, the same simulation conditions were selected. In TOPAS, quadrupole magnet materials were set as air, and the phantom material as water for dose distributions calculations. The scattering effects of air and water on electron beams were considered, resulting in a more accurate maximum dose position induced by VHEE beams focused by the quadrupole magnets. The focusing of the VHEE beams was optimized using dose distribution parameters in a water phantom as the target. This method ensures that the maximum dose is delivered to the precise location.

Using the optimization program, the number of quadrupole magnets was reduced and the beamline was hence simplified. The study shows that three quadrupole magnets, instead of four, are sufficient to focus the 250 MeV VHEE beams to achieve a maximum dose position beyond 17 cm within the phantom. By using three quadrupole magnets to focus 250 MeV VHEE beams, with all components fixed along the beamline, the program allows the position of the maximum dose to be shifted solely by altering the magnetic gradient of the

last quadrupole magnet. This method achieves the positional errors of less than 1%, making the adjustment of treatment depth more convenient and accurate.

The program has been used to spread-out the dose distribution region of the 250 MeV VHEE beams in the water phantom, where the spreading range with flat dose distribution is from 12 to 17 cm along the phantom. By changing the magnetic gradient twice to focus the beams, a flatness of over 99% can be achieved. By setting the magnetic gradients of the last quadrupole magnet in TOPAS according to time characteristics, the simulated SOEP results are in accordance with the calculated results from the program. The lateral dimensions σ_x and σ_y of the dose deposition at the maximum dose position of the spread-out electron peak are both within 1 cm. During lateral scanning irradiation, conformal irradiation can be achieved longitudinally by adjusting the depth range of the SOEP peak position to match the shape of the tumor.

Methods

Focused VHEE

Within the TopasOpt³¹ optimization framework, the parameters and objectives for the NelderMeadOptimiser³² were adjusted to develop a model for focusing VHEE beams. Specifically, the magnetic gradients of the quadrupole magnets (T1 to Tn) and the positions of the components (L1 to Ln+1) were modified. The NelderMeadOptimiser was used to optimize the position of the dose maximum, the dose at the entrance and exit of the water phantom, and the lateral dimensions of dose deposition at the maximum dose. The optimization flowchart is shown in Fig. 5.

Calculate SOEP

Calculate the total dose accumulated from multiple beams in the smallest grids along the central axis

$$D_{total} = \sum_{i=1}^N a_i D_i \quad (1)$$

where D_{total} is the total dose, a_i is a coefficient factor (varied), D_i is the dose (varied), N is the number of beams. In this study, it refers to the total dose within a 0.297 cm × 0.297 cm × 30 cm region along the central axis.

Calculate the mean dose in the spread-out region

$$\langle D \rangle = \frac{1}{N} \sum_{i=1}^N D_i \quad (2)$$

where $\langle D \rangle$ is the mean dose.

Calculate the standard deviation of the dose in the spread-out region

$$\sigma D = \sqrt{\frac{1}{N} \sum_{i=1}^N (D_i - \langle D \rangle)^2} \quad (3)$$

where σD is the standard deviation of dose.

Calculate the flatness of the spread-out region

$$F = \left(1 - \frac{\sigma D}{\langle D \rangle} \right) \times 100 \quad (4)$$

where F is the flatness.

Define the flatness of the spread-out region as total_dose_objective. Data1.csv to Datan.csv are derived from the “Focused VHEE”. The Differential Evolution method³³ was employed to optimize the coefficients a_i and to find the minimum value of the total_dose_objective. The algorithm flow for calculating SOEP is shown in Fig. 6.

TOPAS-SOEP simulation

In TOPAS, the magnetic gradients of the last quadrupole magnet were defined using “Time Features”. One can adjust the time variation of the magnetic gradients based on the beam coefficients obtained from “Calculate SOEP” to calculate the dose distribution.

Monte Carlo simulation details

To enable a comparison with the results achieved using four quadrupole magnets to focus the VHEE beams¹, the same beam parameters were employed. In TOPAS Monte Carlo simulations, the energy of the focused VHEE beams is 250 MeV, with typical parameters for clinical proton beams: initial beam size of $\sigma = 4$ mm following a Gaussian distribution, energy spread of 0.75 MeV, and angular divergence of 3.2 mrad^{1,34}. The sizes of each quadrupole magnet are 40 cm × 40 cm × 24 cm, with the medium set to air in TOPAS. The sizes of the water phantom are 30 cm × 30 cm × 30 cm. The beamline established in TOPAS is shown in Fig. 7. To position the maximum dose at 17 cm, the magnetic gradients and positions of three quadrupole magnets were optimized to focus a 250 MeV VHEE beam. Based on the optimization results, the positions of the components were fixed, and the magnetic gradients of the first two quadrupole magnets were set to T2 and T3 accordingly, while limiting the entrance and exit doses on the central axis of the water phantom to below 25% of the maximum dose. To explore the relationship between the gradient of the last quadrupole magnet and the target position, 50 target positions z' where the maximum dose is located between 9 and 18 cm are randomly selected. The gradient of

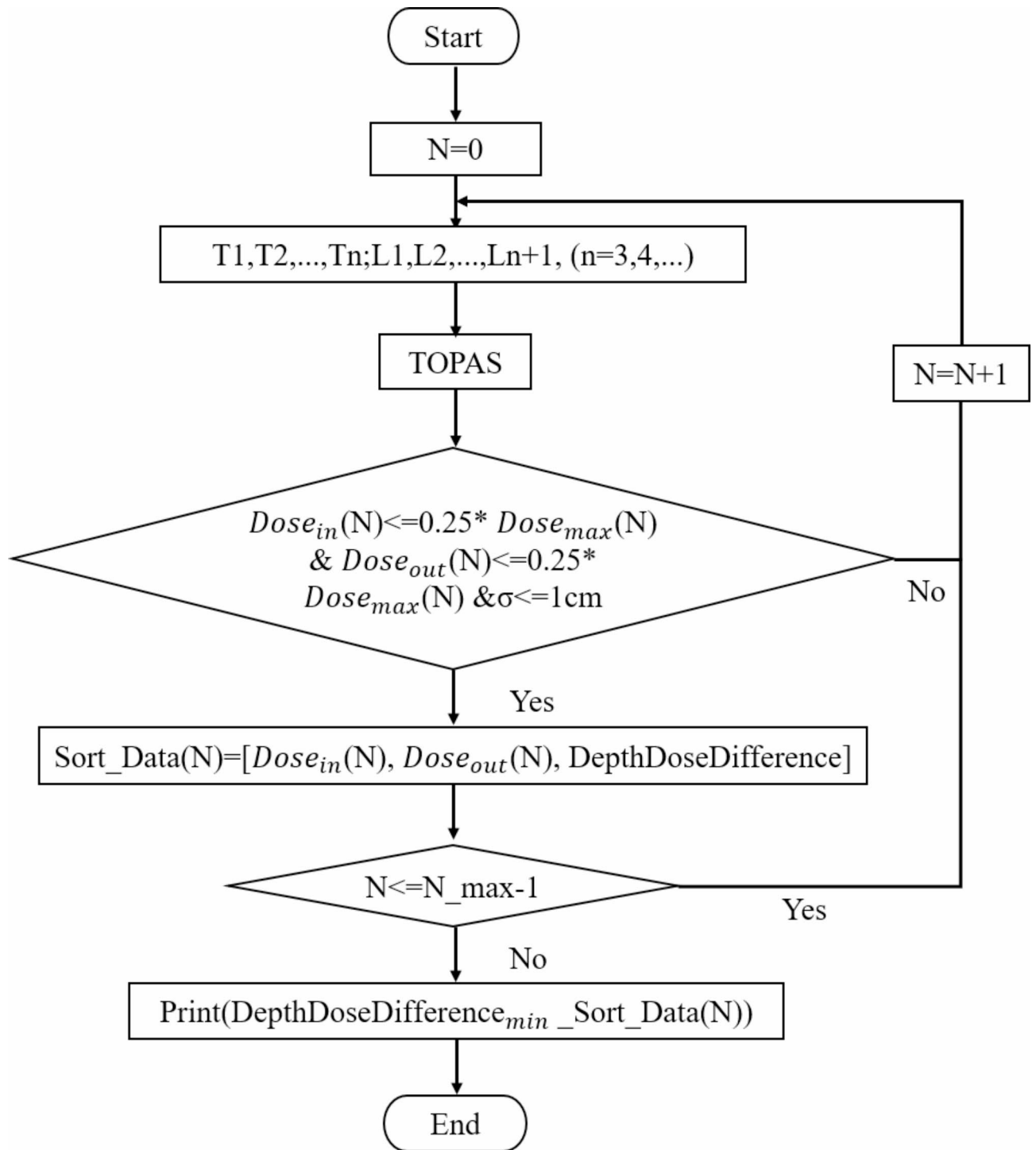


Fig. 5. Flowchart of the algorithm for optimizing focused VHEE.

the last quadrupole magnet was recorded for each position. The target positions were distributed as evenly as possible across the entire range to ensure the reliability of the resulted relationship.

Data processing

Dose distribution data were processed using Origin (Version 2024b, OriginLab Corporation, Northampton, MA, USA). Linear regression was performed to calculate the relationship between the quadrupole magnet gradients and the positions of maximum dose.

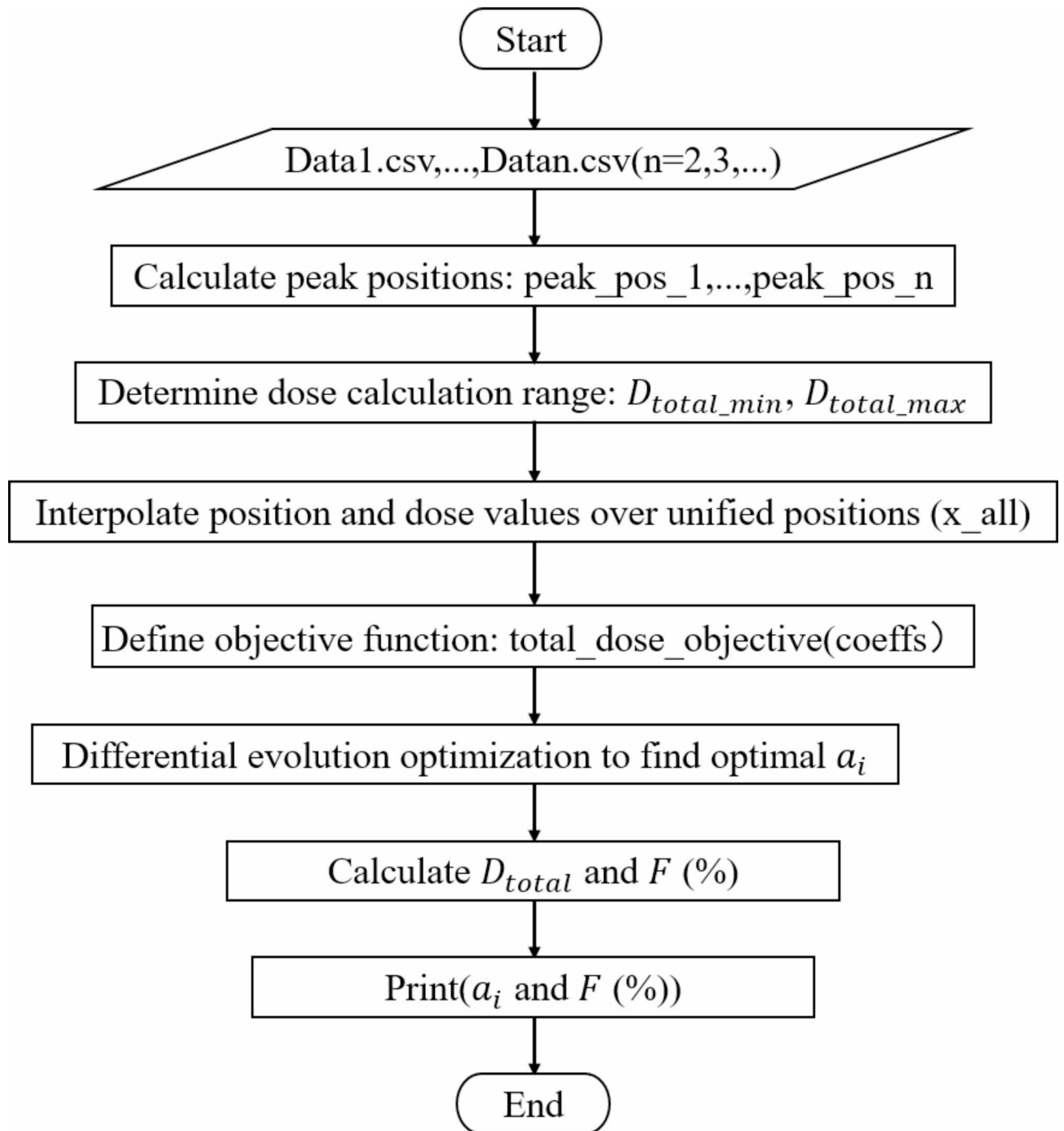


Fig. 6. Flowchart of the algorithm for calculating SOEP.

Dose distributions

In the case of VHEE beams, a grid of $101 \times 101 \times 101$ voxels is set to reduce the computation time for dose distribution calculations using the “scorer”. For all dose distribution calculations related to specific positions in this study, the grid size is uniformly set to $101 \times 101 \times 501$ voxels, dividing the water phantom along the z -axis into 501 voxels. When reading the two-dimensional dose distributions (z - x and z - y), calculations are based on grids of $101 \times 1 \times 501$ voxels ($30 \text{ cm} \times 0.297 \text{ cm} \times 30 \text{ cm}$) and $1 \times 101 \times 501$ voxels ($0.297 \text{ cm} \times 30 \text{ cm} \times 30 \text{ cm}$) respectively. For the cross-sectional x - y dose profile, calculations are based on a grid of $101 \times 101 \times 1$ voxels ($30 \text{ cm} \times 30 \text{ cm} \times 0.05988 \text{ cm}$).

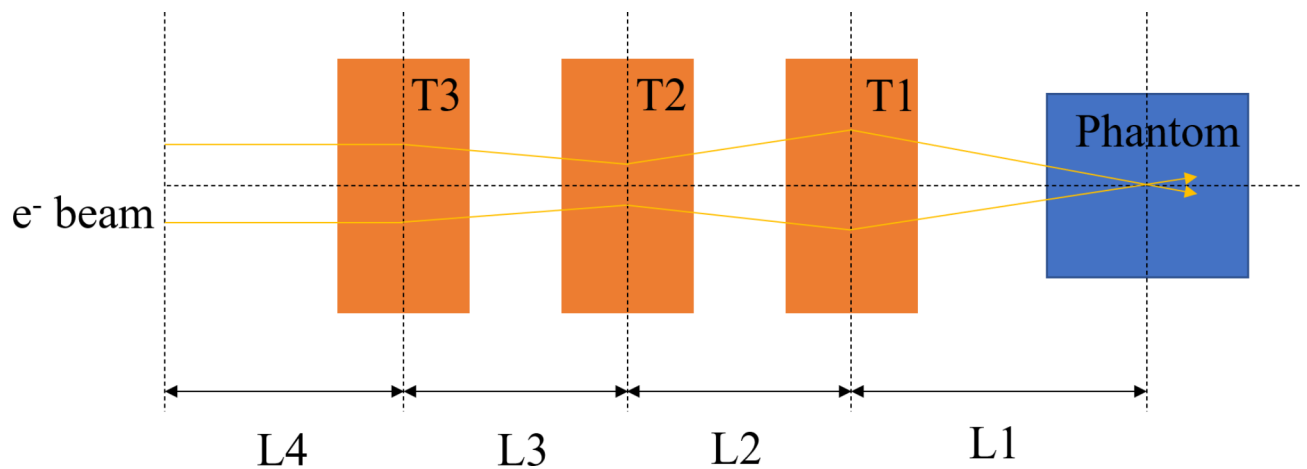


Fig. 7. Beamline established in TOPAS using three quadrupole magnets to focus 250 MeV VHEE beams.

Data availability

The datasets generated during and/or analysed during the current study are available from the corresponding author on reasonable request.

Received: 26 July 2024; Accepted: 6 November 2024

Published online: 11 November 2024

References

- Whitmore, L., Mackay, R. I., van Herk, M., Jones, J. K. & Jones, R. M. Focused VHEE (very high energy electron) beams and dose delivery for radiotherapy applications. *Sci. Rep.* **11**, 14013 (2021).
- DesRosiers, C., Moskvina, V., Bielajew, A. F. & Papiez, L. 150–250 MeV electron beams in radiation therapy. *Phys. Med. Biol.* **45**, 1781 (2000).
- Böhlen, T. T. et al. Very high-energy electron therapy as light-particle alternative to transmission proton FLASH therapy – an evaluation of dosimetric performances. *Radiother. Oncol.* **194**, 110177 (2024).
- Böhlen, T. T. et al. Characteristics of very high-energy electron beams for the irradiation of deep-seated targets. *Med. Phys.* **48**, 3958–3967 (2021).
- Palma, B. et al. MO-FG-303-06: evaluation of the performance of very high-energy Electron (VHEE) beams in Radiotherapy: five clinical cases. *Med. Phys.* **42**, 3568–3568 (2015).
- Palma, B. et al. Assessment of the quality of very high-energy electron radiotherapy planning. *Radiother. Oncol.* **119**, 154–158 (2016).
- Yeboah, C., Sandison, G. A. & Moskvina, V. Optimization of intensity-modulated very high energy (50–250 MeV) electron therapy. *Phys. Med. Biol.* **47**, 1285 (2002).
- Bazalova-Carter, M. et al. Treatment planning for radiotherapy with very high-energy electron beams and comparison of VHEE and VMAT plans. *Med. Phys.* **42**, 2615–2625 (2015).
- Kokurewicz, K. et al. Focused very high-energy electron beams as a novel radiotherapy modality for producing high-dose volumetric elements. *Sci. Rep.* **9**, 10837 (2019).
- Papiez, L., DesRosiers, C. & Moskvina, V. Very high energy electrons (50–250 MeV) and radiation therapy. *Technol. Cancer Res. Treat.* **1**, 105–110 (2002).
- Lagzda, A. et al. Relative Insensitivity to Inhomogeneities on Very High Energy Electron Dose Distributions. (2017). <https://doi.org/10.18429/JACoW-IPAC2017-THPVA139>
- Böhlen, T. T. et al. Normal tissue sparing by FLASH as a function of single-fraction dose: a quantitative analysis. *Int. J. Radiat. Oncol. Biol. Phys.* **114**, 1032–1044 (2022).
- No, H. J. et al. Clinical LINAC-Based Electron FLASH: pathway for practical translation to trials of FLASH Radiotherapy. *Int. J. Radiation Oncology*Biophysics*. **114**, e539 (2022).
- Böhlen, T. T. et al. Effect of Conventional and Ultrahigh Dose Rate FLASH irradiations on Preclinical Tumor models: a systematic analysis. *Int. J. Radiation Oncology*Biophysics*. **117**, 1007–1017 (2023).
- Valdés Zayas, A. et al. Independent Reproduction of the FLASH Effect on the gastrointestinal tract: a multi-institutional comparative study. *Cancers*. **15**, 2121 (2023).
- Vozenin, M. C., Bourhis, J. & Durante, M. Towards clinical translation of FLASH radiotherapy. *Nat. Reviews Clin. Oncol.* **19**, 791–803 (2022).
- Lin, B. et al. FLASH Radiotherapy: history and future. *Front. Oncol.* **11**, 644400 (2021).
- Lin, X. C. et al. A compact X-band backward traveling-wave accelerating structure. *Nucl. Sci. Tech.* **35**, 40 (2024).
- Zhang, G., Zhang, Z., Gao, W. & Quan, H. Treatment planning consideration for very high-energy electron FLASH radiotherapy. *Phys. Medica-European J. Med. Phys.* **107**, 102539 (2023).
- Whitmore, L. et al. CERN-based experiments and Monte-Carlo studies on focused dose delivery with very high energy electron (VHEE) beams for radiotherapy applications. *Sci. Rep.* **14**, 11120 (2024).
- Krim, D., Rrhioua, A., Zerfaoui, M. & Bakari, D. Monte Carlo modeling of focused Very High Energy Electron beams as an innovative modality for radiotherapy application. *Nucl. Instrum. Methods Phys. Res., Sect. A.* **1047**, 167785 (2023).
- Kokurewicz, K. et al. An experimental study of focused very high energy electron beams for radiotherapy. *Commun. Phys.* **4**, 33 (2021).
- Kang, M., Wei, S., Choi, J. I., Simone, C. B., Lin, H. & 2nd & Quantitative Assessment of 3D dose rate for Proton Pencil Beam Scanning FLASH Radiotherapy and its application for Lung Hypofractionation Treatment Planning. *Cancers (Basel)*. **13**, 3549 (2021).

24. Schwarz, M., Traneus, E., Safai, S., Kolano, A. & van de Water Treatment planning for Flash radiotherapy: General aspects and applications to proton beams. *Med. Phys.* **49**, 2861–2874 (2022).
25. Schüller, E. et al. Very high-energy electron (VHEE) beams in radiation therapy; treatment plan comparison between VHEE, VMAT, and PPBS. *Med. Phys.* **44**, 2544–2555 (2017).
26. Bortfeld, T. & Schlegel, W. An analytical approximation of depth-dose distributions for therapeutic proton beams. *Phys. Med. Biol.* **41**, 1331–1339 (1996).
27. Borland, M. Elegant: a flexible SDDS-compliant code for accelerator simulation. (2000). <https://doi.org/10.2172/761286>
28. Wiedemann, H. *Particle Accelerator Physics* (Springer Cham, 2015). <https://doi.org/10.1007/978-3-319-18317-6>
29. Perl, J., Shin, J., Schumann, J., Faddegon, B. & Paganetti, H. TOPAS: an innovative proton Monte Carlo platform for research and clinical applications. *Med. Phys.* **39**, 6818–6837 (2012).
30. Rahman, M. et al. FLASH radiotherapy treatment planning and models for electron beams. *Radiother. Oncol.* **175**, 210–221 (2022).
31. Whelan, B., Loo, B. W. Jr, Wang, J. & Keall, P. TopasOpt: an open-source library for optimization with Topas Monte Carlo. *Med. Phys.* **50**, 1121–1131 (2023).
32. Chang, C. W. & Chang, J. S. K. Option pricing with stochastic volatility: information-time vs. calendar-time. *Manage. Sci.* **42**, 974–991 (1996).
33. Qiang, J. & Mitchell, C. E. A unified Differential Evolution Algorithm for Global optimization. *IEEE Trans. Evol. Comput.* (2014). <https://cloudfront.escholarship.org/dist/prd/content/qt41b84414/qt41b84414.pdf?t=nf9gvi>
34. Paganetti, H., Jiang, H., Parodi, K., Slopesma, R. & Engelsman, M. Clinical implementation of full Monte Carlo dose calculation in proton beam therapy. *Phys. Med. Biol.* **53**, 4825–4853 (2008).

Acknowledgements

This work was supported by the National Natural Science Foundation of China (No. 12275196) and the Major Science and Technology Project of Hubei Province, China (No. 2021AFB001). Special thanks to the Institute for Advanced Studies at Wuhan University for its support with the Monte Carlo simulations. We also appreciate L.X Liu and J.H Zhong from the same group for their valuable discussions during the research period.

Author contributions

C.A. performed the optimization program code development, simulations with TOPAS, and data processing and analysis, with contributions to the conceptual development of the work by all authors. C. A., W. Z., Z.D., J.L., X. Y., J. W. and Y.N. contributed to writing the manuscript. Y. N. provided overall supervision.

Fundings

This work was supported by the National Natural Science Foundation of China (No. 12275196) and the Major Science and Technology Project of Hubei Province, China (No. 2021AFB001).

Declarations

Competing interests

The authors declare no competing interests.

Additional information

Supplementary Information The online version contains supplementary material available at <https://doi.org/10.1038/s41598-024-79187-4>.

Correspondence and requests for materials should be addressed to Y.N.

Reprints and permissions information is available at www.nature.com/reprints.

Publisher's note Springer Nature remains neutral with regard to jurisdictional claims in published maps and institutional affiliations.

Open Access This article is licensed under a Creative Commons Attribution-NonCommercial-NoDerivatives 4.0 International License, which permits any non-commercial use, sharing, distribution and reproduction in any medium or format, as long as you give appropriate credit to the original author(s) and the source, provide a link to the Creative Commons licence, and indicate if you modified the licensed material. You do not have permission under this licence to share adapted material derived from this article or parts of it. The images or other third party material in this article are included in the article's Creative Commons licence, unless indicated otherwise in a credit line to the material. If material is not included in the article's Creative Commons licence and your intended use is not permitted by statutory regulation or exceeds the permitted use, you will need to obtain permission directly from the copyright holder. To view a copy of this licence, visit <http://creativecommons.org/licenses/by-nc-nd/4.0/>.

© The Author(s) 2024